

Low Latency Temporal Filter Design for Real-Time MRI Using UNFOLD

Peter Kellman,* Jonathan M. Sorger, Frederick H. Epstein, and Elliot R. McVeigh

To improve real-time control of interventional procedures such as guidance of catheters, monitoring of ablation therapy, or control of dosage during drug delivery, the image acquisition and reconstruction must be high speed and have low latency (small time delay) in processing. A number of different methods have been demonstrated which increase the speed of MR acquisition by decreasing the number of sequential phase-encodes. A design and implementation of the UNFOLD method which achieves the desired low latency with a recursive temporal filter is presented. The recursive filter design is characterized for this application and compared with more commonly used moving average filters. Experimental results demonstrate low-latency UNFOLD for two applications: 1) high-speed, real-time imaging of the heart to be used in conjunction with cardiac interventional procedures; and 2) the injection of drugs into muscle tissue with contrast enhancement, i.e., monitoring needle insertion and injection of a drug with contrast enhancement properties. Proof-of-concept was demonstrated by injecting a contrast agent. In both applications the UNFOLD technique was used to double the frame rate. Magn Reson Med 44:933–939, 2000. © 2000 Wiley-Liss, Inc.

Key words: interventional MR; UNFOLD; rapid imaging; real-time imaging; cardiac imaging

Real-time MRI has now achieved the spatial and temporal resolution necessary for monitoring interventions (1). To improve real-time control of interventional procedures such as guidance of catheters, monitoring of ablation therapy, and control of dosage during drug delivery, the image acquisition and reconstruction must be high speed and have low latency (small time delay) in processing. A number of different methods (2,3) have been demonstrated which increase the speed of MR acquisition by decreasing the number of sequential phase-encodes. The UNFOLD technique (2) is based on time interleaving of k -space lines in sequential images and exploits the fact that the outer portion of the FOV is relatively static. The SENSE technique (3) exploits the differences in spatial sensitivity of multiple receiver coils to eliminate the aliased component that results from undersampling k -space.

Application of the UNFOLD method to retrospective cine imaging of the heart has been described (2). In this paper, we describe a modified temporal filter designed specifically for applications demanding low latency. In non-breath-held applications, such as interventional MRI, the assumption made by UNFOLD that the outer portion of the FOV is relatively static is not always met, particularly

if chest wall motion occurs. As a result, alias artifacts are not perfectly removed. We analyze this issue in greater detail, present an example filter design, and discuss design tradeoffs between desired temporal bandwidth and alias artifact rejection. We present a design and implementation of the UNFOLD method which achieves the desired low latency with a recursive temporal filter. The recursive filter design is characterized for this application and compared with more commonly used moving average filters.

We present experimental results that demonstrate low-latency UNFOLD for two applications. The first application is high-speed, real-time imaging of the heart to be used in conjunction with cardiac interventional procedures such as angioplasty, catheter ablation, or injection of drugs into the myocardium. This demonstration involved imaging without an interventional procedure. The second application is injection of drugs into muscle tissue with contrast enhancement, i.e., monitoring needle insertion and injection of a drug with contrast enhancement properties. Proof-of-concept was demonstrated by injecting a contrast agent. In both applications the UNFOLD technique was used to double the frame rate.

METHODS

UNFOLD Method

The UNFOLD technique (2) is based on acquiring k -space phase-encode lines in a time-interleaved fashion, i.e., the sequence acquisition alternates even and odd lines to increase the frame rate by a factor of $R = 2$. The images reconstructed from either the even or odd lines have aliasing, which results from halving the FOV. The sign of the aliased component is alternating; thus the aliased component is shifted in temporal frequency and may be rejected by means of low-pass temporal filtering.

For a sequence of images, $f(x, y, t)$, with corresponding spatial Fourier transform (k -space data) $F(k_x, k_y, t)$, the sampled k -space data and reconstructed images are a Fourier pair, which may be written as:

$$F(k_x, k_y, t) \times (1/\Delta k) \text{comb}(k_y/\Delta k) \Leftrightarrow f(x, y, t) * \text{comb}(y/\text{FOV}), \quad [1]$$

where Δk corresponds to the sample spacing along k_y for a full unaliased FOV = $(1/\Delta k)$, and the asterisk denotes the convolution operation. For $R = 2$ UNFOLD, the sample spacing is increased to $2 \Delta k$. In this case, the phase of the aliased images is a linear function of the k -space sampling offset, δk . The Fourier pair may be written as:

$$F(k_x, k_y, t) \times (1/2\Delta k) \text{comb}[(k_y - \delta k)/2\Delta k] \Leftrightarrow f(x, y, t) * \{\text{comb}(y/\text{FOV}/2)e^{-j2\pi\delta k y}\}, \quad [2]$$

Laboratory of Cardiac Energetics, National Institutes of Health, National Heart, Lung, and Blood Institute, Bethesda, Maryland.

*Correspondence to: Peter Kellman, Laboratory of Cardiac Energetics, National Institutes of Health, National Heart, Lung, and Blood Institute, 10 Center Drive, MSC-1061, Building 10, Room B1D416, Bethesda, MD 20892-1061. E-mail: kellman@nih.gov

Received 4 April 2000; revised 19 June 2000; accepted 5 July 2000.

© 2000 Wiley-Liss, Inc.

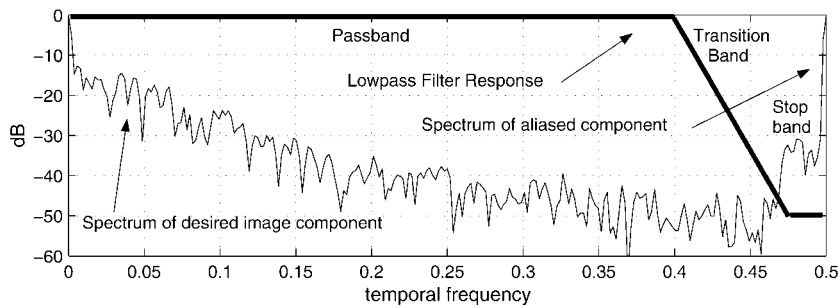


FIG. 1. Illustration of temporal spectrum of a pixel showing both desired and alias pixel components, with low-pass temporal filter response overlaid.

where the sampling offset δk alternates between 0 and Δk for acquisition of even and odd lines. For $R = 2$ UNFOLD, the phase shift of the aliased image centered at $y = \text{FOV}/2$ alternates between 0 and $2\pi\delta k \text{FOV}/2 = \pi$. Within the FOV, the sequence of images may be written more simply as:

$$f(x, y, t) + (-1)^t [f(x, y - \text{FOV}/2, t) + f(x, y + \text{FOV}/2, t)], \quad [3]$$

where $t = 0, 1, 2, \dots$ is a discrete time index and provided there is no aliasing within the full FOV, i.e., $f(x, y, t) = 0$ outside the FOV.

The principle of UNFOLD is to separate the desired component, $f(x, y, t)$, from the undesired aliased component, $f(x, y \pm \text{FOV}/2)(-1)^t$ by means of low-pass temporal filtering. Each pixel is comprised of two components that share the same bandwidth. The aliased component has been shifted to the band edge and can be rejected by means of low-pass temporal filtering. More bandwidth can be allocated to the desired image component if the aliased image region is relatively static with correspondingly less temporal bandwidth. For example, if the dynamic region is restricted to the center half of the FOV, and if the top and bottom quarters of the FOV (which alias into the center) are relatively static, then the bandwidth or low-pass cutoff can be selected to give greater bandwidth to the desired central region. Figure 1 illustrates temporal spectra of an image pixel for a simulated example. In Fig. 1, the spectral components of the aliased pixel have been shifted by 0.5 (normalized to the sample rate) due to the interleaved acquisition, and have a lower bandwidth relative to the desired component, based on the assumption that the aliased region is relatively static. The magnitude response of a specific temporal filter (to be discussed later) is overlaid for comparison.

As an example, in cardiac MR applications in which the beating heart is in the central portion of the FOV, and the back and chest are at the edges of the FOV, the temporal bandwidth of the back and chest are less than that of the beating heart, and therefore may be rejected by low-pass filtering, in which most of the temporal bandwidth can be used to pass the heart motion. This assumption is reasonably valid provided the sampling rate is sufficiently high.

Temporal Filter Design and Characterization

Design criteria for the temporal low-pass filter used in the UNFOLD application include standard spectral response measures such as bandwidth, passband ripple, stopband

rejection, and group delay and distortion, as well as temporal characteristics such as the impulse and step responses. For a given application, it is important to translate the required imaging performance into these design parameters. For applications such as interventional MRI involving real-time control, it is important to minimize the delay or latency in the reconstruction. Assuming that the computation involved in reconstruction is not a limiting factor, then the latency inherent in the temporal filter will ultimately determine the minimum delay.

To design the temporal low-pass filter it is necessary to first specify the passband and the stopband. While the width of the filter impulse response (at half power) is inversely proportional to the passband bandwidth, the impulse response is actually much longer in duration due to the small transition band between the passband and stopband. For low-pass filter designs based on moving average (finite impulse response) with symmetric weighting, the longer duration impulse response, which results from a sharp filter (narrow transition band), translates directly into a long latency. However, by using a recursive filter, the impulse response is asymmetric and the latency is very small. The criteria for passband and stopband specification and filter performance and design tradeoffs are presented in the following.

Performance measures such as bandwidth and stopband rejection depend on image content and degree of motion, and are thus difficult to specify. In practice, it is often necessary to optimize the final parameters empirically; nevertheless, insight is gained by considering an example. First, specify the stopband rejection and cut-off required to eliminate the aliased component (based on the temporal bandwidth of this component). After steady state magnetization of the tissue (e.g., chest and heart) is reached, the temporal bandwidth of the aliased component due to the region at the periphery of the FOV is typically determined by chest wall motion resulting from breathing (unless breath-held imaging is used). In interventional MRI applications it may also include motion of the catheter or other device. Blood flow in vessels at the edge of the FOV may also contribute.

In this design example, assume that the temporal bandwidth of pixels in the aliased region is a result of chest motion. Chest wall motion has a large, relatively slow component due to breathing, and a smaller, higher-rate, more impulsive component caused by the motion of the beating heart (4). It is necessary to determine the bandwidth of these undesired components to specify the filter stopband. In general, the temporal signal $f(x, y, t)$ for a

given pixel is a complex signal with both amplitude and phase, the latter resulting from off-resonance effects and flow or motion. The resulting temporal bandwidth of the chest wall motion is proportional to the rate of motion and the depth of modulation, i.e., larger phase modulation increases the temporal bandwidth. The degree or depth of phase modulation is a complex function of many variables. The chest wall velocity and the gradient in the local field inhomogeneity are both low. The dominant source of phase modulation in this example arises due to the off-resonance of chemical shift, which changes in pixels at the moving boundary between fat and water.

For cardiac applications using surface coils, the chest wall signal is very strong; therefore, a large stopband attenuation is required to suppress these spectral components. The aliased components are shifted in temporal frequency to the band edge due to the interleaved k -space sampling used in the UNFOLD method. A stopband frequency of $f_{\text{sample}}/2 - f_h$ is required to suppress the fundamental frequency of the heart rate-induced chest wall motion, where f_{sample} is the temporal sample rate (image frame rate) and f_h is the heart rate. For example, with a heart rate of 60 bpm (1 Hz) and a frame rate of 30 frames/sec, a stopband frequency of 14 Hz is required. It may be necessary to lower the stopband cutoff to suppress additional harmonics due to the impulsive nature of the heart rate motion.

The stopband rejection must be sufficient to attenuate the aliased components to a level below the noise. For a maximum signal-to-noise ratio (SNR) of 40 dB (reasonable at the stated 30 frames/sec), a stopband rejection of 50 dB will ensure that the alias artifact is below the noise. For digital filter design, the stopband frequency is first normalized by the sample rate. In this example, using 30 frames/sec real-time imaging, a stopband of 14 Hz equates to a normalized stopband frequency of $14/30 \sim 0.47$ (normalized by sample rate).

Given the specifications for the stopband frequency and rejection, it is necessary to specify passband cutoff (and flatness), which will determine the transition band. These parameters, together with the filter type and order, will determine the overall response. The filter order will be dictated by the transition bandwidth in a reciprocal relationship (i.e., a smaller transition band requiring a larger filter order). If the narrow transition band causes unacceptable distortion in impulse or step response, it may be necessary to reduce the effective temporal resolution (by decreasing the passband cutoff) or, if possible, increase the sample rate. The level of acceptable distortion will depend heavily on the application. For instance, quantitative analysis of the time intensity curves to determine regional uniformity of contrast enhancement will place more stringent requirements on the temporal response than real-time feedback for control of catheter position.

In this design example, choose a passband cut-off of 0.4 (normalized to the sample rate), corresponding to 80% of the available bandwidth. This is a somewhat arbitrary tradeoff. A much lower cut-off defeats the purpose of using UNFOLD to gain a twofold increase in speed, and increasing the cut-off has diminishing returns and begins to increase the filter order rapidly (as transition band decreases). A flatness gain of 1.5 dB within the passband was

specified (again somewhat arbitrarily). Summarizing the magnitude frequency response specification: $f_p = 0.4$ (passband cutoff), $R_p = 1.5$ dB (passband flatness), $f_s = 0.47$ (stopband frequency), $R_s = 50$ dB (stopband rejection), with all frequencies normalized by the sample rate.

There are a number of digital filter designs with various attributes (5). It is common to use a symmetric, finite impulse response (FIR) filter, also referred to as a moving average, which has linear phase characteristics and thus no delay distortion. However, the FIR design may have considerable latency. Recursive filters, known as infinite impulse response (IIR) filters, may be used, which will reduce the latency but will introduce some non-linear phase (vs. frequency) or delay distortion, typically at the passband edge. The overall temporal distortion due to both non-linear phase and truncation of the signal spectrum is characterized by the impulse response. Group delay distortion may broaden the impulse response and contribute to "ringing." In this specific design example, the IIR filter design has relatively low delay distortion, and the impulse response for both IIR and FIR designs have comparable duration and "ringing."

For real-time, low-latency applications (discussed in the Results section) an elliptical IIR design was selected. The elliptic filter met the desired magnitude response with a lower order than either the Chebyshev or Butterworth designs (5), and had comparable delay distortion over 90% of the passband. The filter implementation chosen was a "Direct Form II Transposed" form, which is based on the standard difference equation:

$$a(1)g(t) = b(1)f(t) + b(2)f(t-1) + \dots \\ + b(N_b + 1)f(t - N_b) - a(2)g(t-1) - \dots \\ - a(N_a + 1)g(t - N_a) \quad [4]$$

where $f(t)$ is the discrete time sampled input signal for each pixel (i.e., $f(x, y, t)$), $g(t)$ is the temporally filtered output, and N_a and N_b are the length of the autoregressive and moving average filter coefficients, respectively. To meet the example design specifications, using an elliptical filter, $N_a = N_b = 3$, and $a(1) = 1$.

Experimental Parameters

All results were obtained using a GE Signa CV 1.5 Tesla MR Imager using a real-time fast gradient recalled echo train (FGRE-ET) pulse sequence (6). Imaging was performed using the real-time FGRE-ET pulse sequence with UNFOLD, and data was reconstructed using the low-latency temporal filter described above ($N = 3$ elliptic IIR, with $R_p = 1.5$, $R_s = 50$, $f_p = 0.4$, and $f_s = 0.47$). Reconstruction was performed off-line. A real-time on-line system is in development.

Cardiac imaging of a short axis slice was performed at 31.2 frames/sec using the following parameters: echo train length (ETL) = 8 echoes; bandwidth = ± 125 kHz; TR = 10.7 msec; flip angle = 15°; and slice thickness = 10 mm. The FOV was 400 mm \times 200 mm (1/2 FOV) with an image resolution of 128 frequency-encodes \times 128 phase-encodes. There were 48 k -space lines acquired for 1/2 FOV and 3/4 NEX partial k -space acquisition. Using UNFOLD, the

48 phase-encodes were acquired in an interleaved manner: 24 odd lines followed by 24 even, and so on. Thus each of the 24 phase-encodes were acquired in 3 TRs, resulting in a frame period of $3 \times 10.7 = 32.1$ msec (approximately 31.2 frames/sec). The real-time sequence was continuous (i.e., not triggered). A cardiac phased array comprised of 4 surface coils was used. The complex images were temporally filtered for each coil individually prior to magnitude combining.

A proof-of-concept experiment to demonstrate needle guidance for contrast-enhanced drug delivery was performed by injecting gadopentetate dimeglumine (Magnevist) directly into muscle tissue. The subject of this experiment was a rabbit, and the experiment was conducted in accordance with protocols approved by the Animal Care and Use Committee of the National Institutes of Health. An injection was made into the sacrospinalis (back) muscle while imaging an axial slice containing the needle. The parameters used for this proof-of-concept experiment differed from those used in the cardiac application due to the small FOV.

The parameters for this second experiment were as follows: echo train length (ETL) = 8 echoes; ± 125 kHz bandwidth; flip angle = 15° ; slice thickness = 10 mm. The FOV was $150\text{mm} \times 112.5\text{mm}$ ($3/4$ FOV) with an image resolution of 128 frequency-encodes \times 96 phase-encodes. There were 64 k -space lines acquired for $3/4$ FOV and partial k -space acquisition with 28 overscan lines. Using UNFOLD, the 64 phase-encodes were acquired in an interleaved manner: 32 odd lines followed by 32 even, and so on. Due to gradient duty cycle limits imposed by the scanner for the small FOV selected, $\text{TR} = 31.2$ msec. Thus each of the 32 phase-encodes were acquired in 4 TRs, resulting in a frame period of 4×31.2 msec (approximately 8 frames/sec). The imaging speed would double to 16 frames/sec using a slightly larger FOV which did not have minimum TR constraints. The real-time sequence was continuous (i.e., not triggered). A phased array comprised of two surface coils was used.

The injection used a 0.65-mm-diameter (22 gauge) MR-compatible titanium needle (Unimed, S.A, Lausanne, Switzerland). The concentration of contrast agent was 0.625 mmol/L.

RESULTS

Filter Characteristics

Filter characteristics for the elliptic IIR are shown in Fig. 2. By design, the filter meets the magnitude response specification. The IIR filter with its asymmetric response has a group delay (latency) of approximately 0.5 samples corresponding to 17 msec, which is very suitable for real-time applications. The minimum length FIR filter to meet the desired specification was an equiripple design using 23 coefficients designed by the Parks-McClellan method (7) (window designs required 35–45 coefficients, depending on the specific window used). The FIR has a symmetric impulse response; therefore, for 23 coefficients the net delay is 11.5 samples. For real-time imaging at the specified frame rate of 30 frames/sec, this implies a minimum latency of $11.5/30 \approx 0.4$ sec (ignoring any delay due to

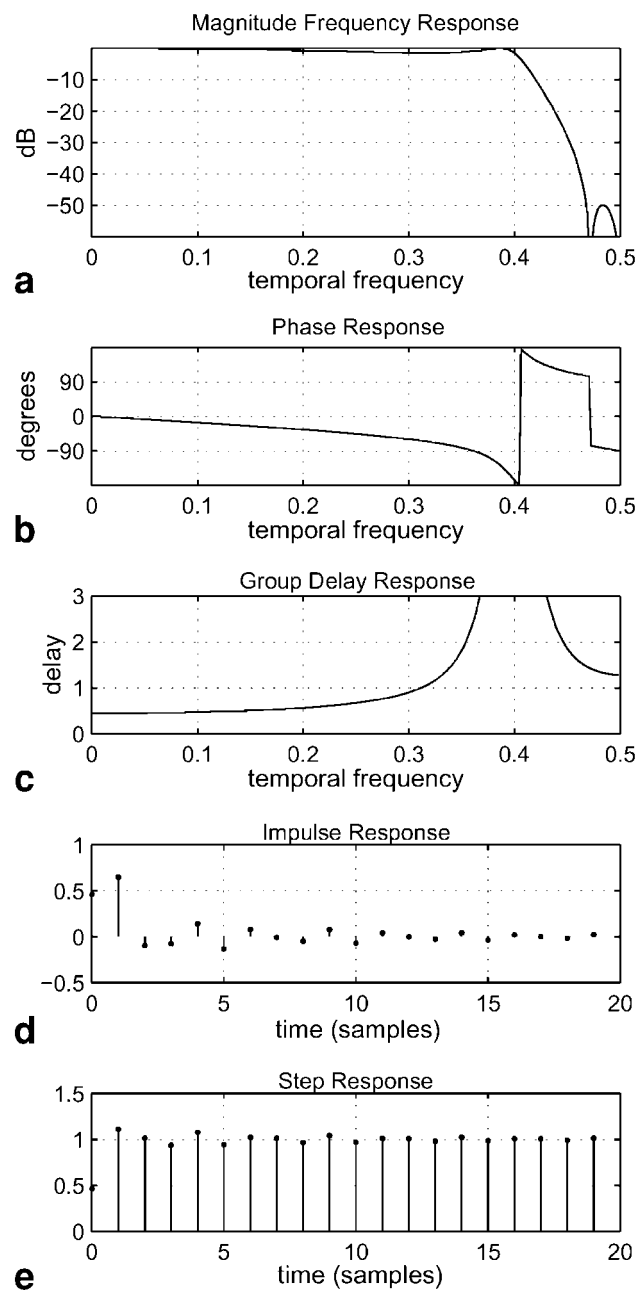


FIG. 2. Low-pass filter response for elliptic IIR design (a) magnitude frequency response, (b) phase response, (c) group delay response, (d) impulse response, and (e) step response.

computation). While the FIR has linear phase and consequently no delay distortion, the step response for both designs is quite comparable, with similar effective duration and overshoot of approximately 10%.

The loss in SNR using UNFOLD as compared to full k -space reconstruction acquired at half the rate (twice the time) is equal to $[(B_n/f_s) \times 2]^{1/2}$, where $B_n = \int |H(f)|^2 df / |H(0)|^2$ is the equivalent noise bandwidth (two-sided) of the filter $H(f)$, and f_s is the sample rate. The elliptic filter described above has a noise bandwidth of $0.71 f_s$ calculated by numerical integration; therefore, the SNR loss factor is 1.2 in this case. The SNR loss of UNFOLD was

validated experimentally using a water phantom. The mean and standard deviation were calculated using 256 image frames. The measured SNR loss factor was within 1% of that predicted.

Cardiac Example

Real-time cardiac imaging will be required for interventional procedures in the heart. In this example we show that real-time cardiac MRI is possible with low latency. An interventional procedure was not performed.

For the cardiac imaging application, an example image is shown in Fig. 3. Figure 3a illustrates the aliased reconstruction before applying the UNFOLD temporal filter, and Fig. 3b shows a filtered image corresponding to the same time. The chest wall artifact has been effectively removed. The temporal spectrum of an aliased pixel in the chest wall is shown in Fig. 4 for a single coil, with the magnitude frequency response of the temporal filter overlaid for reference. The average chest wall component is very strong due to the proximity to the surface coil. The fundamental component of heart rate modulation at approximately

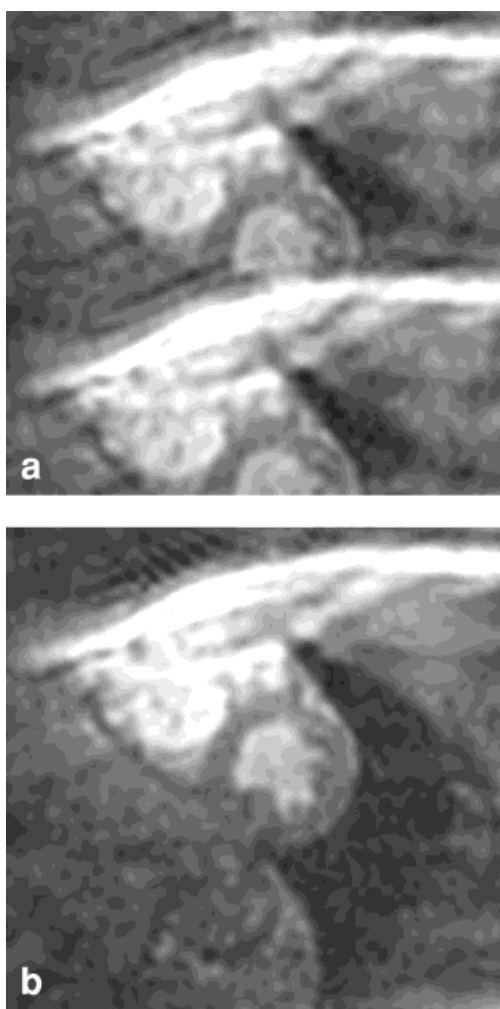


FIG. 3. Cardiac short axis imaging example showing (a) aliased image prior to UNFOLD temporal filter, and (b) UNFOLDED image after temporal filter with alias image rejected.

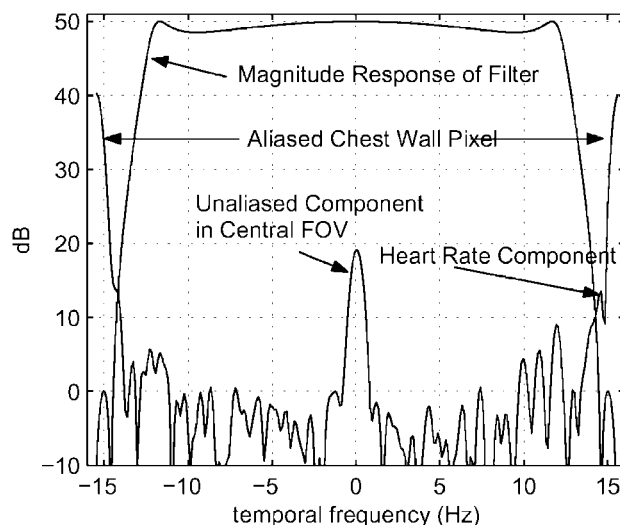


FIG. 4. Temporal spectrum of aliased chest wall pixel with magnitude response of UNFOLD temporal filter overlaid.

± 14.5 Hz, although 25 dB below the average chest wall intensity is also significant. This component is rejected by the temporal filter. Additional harmonics of the heart rate chest wall modulation are evident within the transition band and passband, and contribute to slight artifacts in some of the images. These occur at mid-diastole when the heart is undergoing its maximum rate of expansion. In this example, the subject is in a conventional supine position and the short axis image is doubly oblique, oriented with frequency readout horizontally along the major axis and phase-encode oriented vertically along the minor axis (through the back and chest).

Needle Guidance Example

A sequence of images showing the insertion of the needle, injection of the contrast agent, and withdrawal of the needle is shown in Fig. 5. The still images displayed in Fig. 5 are taken every fourth frame ($\frac{1}{2}$ -sec interval) and have been slightly time-averaged to reduce noise using a boxcar (uniform temporal weighting) of four frames ($\frac{1}{2}$ sec). Averaging was not required for real-time visualization. The needle creates a void and artifact which is well defined and is readily observable. In Fig. 5a–e the needle is being inserted with continuous motion. These images show fine manipulation of the needle is possible to avoid both the spine and the aorta (indicated in Fig. 6a). The contrast agent is injected (lower right of image) during the time period corresponding to Fig. 5f–h, and then the needle is withdrawn in Fig. 5i–l. Figure 6a shows a region into which contrast agent has been injected. The tissue in the region of the injection moves as the needle is withdrawn, so an elliptical ROI was used for the purpose of this example. The average time-intensity-curve for this region is shown in Fig. 6b. The average contrast enhancement in this region was approximately 50%.

The respiration rate of the rabbit (approximately 30 breaths/min) is almost double that for humans, and the heart rate is approximately triple. Furthermore, the tem-

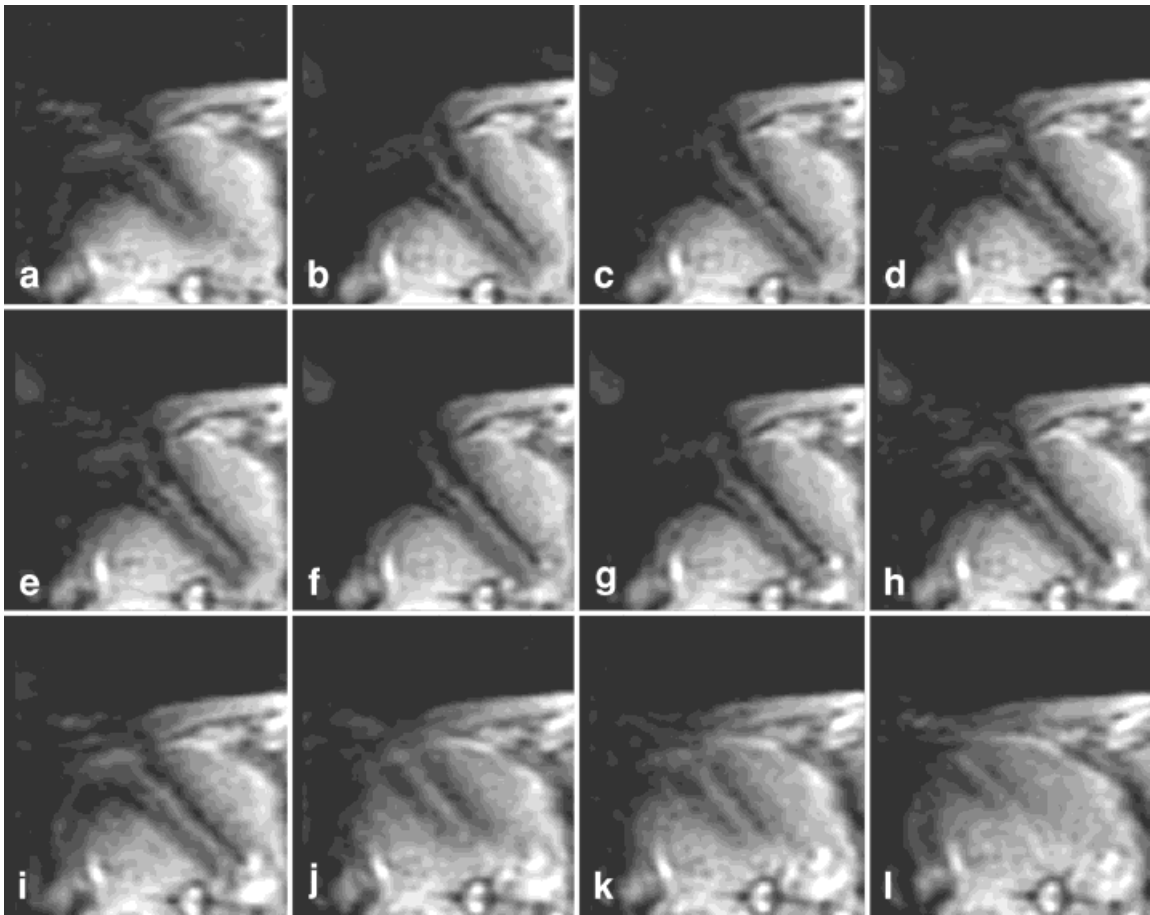


FIG. 5. Image sequence during injection of contrast agent showing: (a–e) needle insertion, (f–h) injection of contrast agent (lower right of image), and (i–l) withdrawal of needle.

poral resolution in this experiment was poorer than in the design example. These factors result in a wider fractional bandwidth of the alias component (relative to the image frame rate). Fortunately, the back muscle did not exhibit

heart-induced motion, as in the cardiac example. As a result, the dominant aliased component due to respiration is at 3.5 Hz (normalized frequency of 0.44), which is in the transition band. The UNFOLD filter was able to effectively

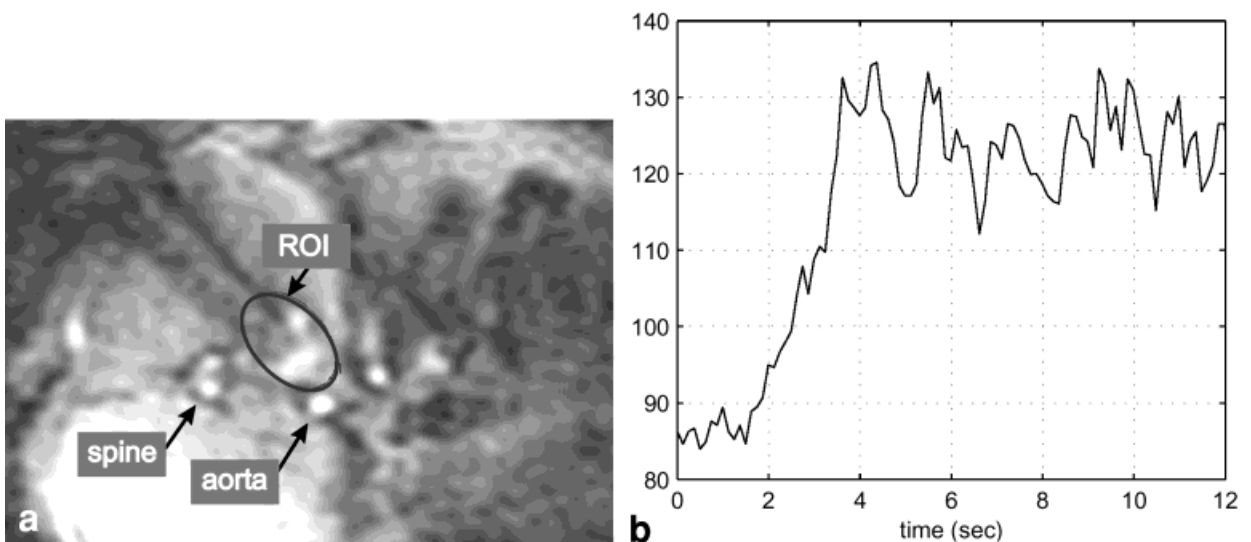
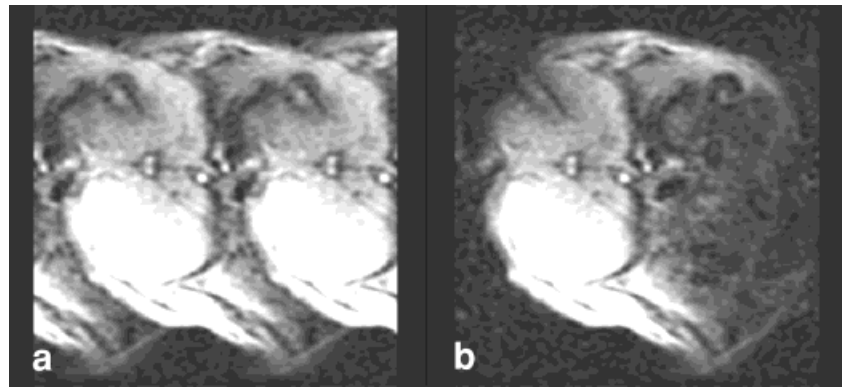


FIG. 6. **a**: ROI with injected contrast agent; **b**: time intensity curve showing contrast enhancement in ROI where contrast agent was injected.

FIG. 7. **a:** Aliased image prior to UNFOLD temporal filter; **b:** UNFOLDED image after temporal filter with alias image rejected.



reject the aliased components, although a slight artifact was evident in some images. Figure 7a shows a reconstructed image before applying the UNFOLD temporal filter, and Fig. 7b shows a filtered image corresponding to the same time. The temporal spectrum of an aliased pixel is shown in Fig. 8 for a single coil, with the magnitude frequency response of the temporal filter overlaid for reference. The UNFOLD method was particularly useful in this case, in which a longer TR resulted from such a small FOV.

CONCLUSIONS

The implementation of UNFOLD with low-latency temporal filtering has been demonstrated in cases which have

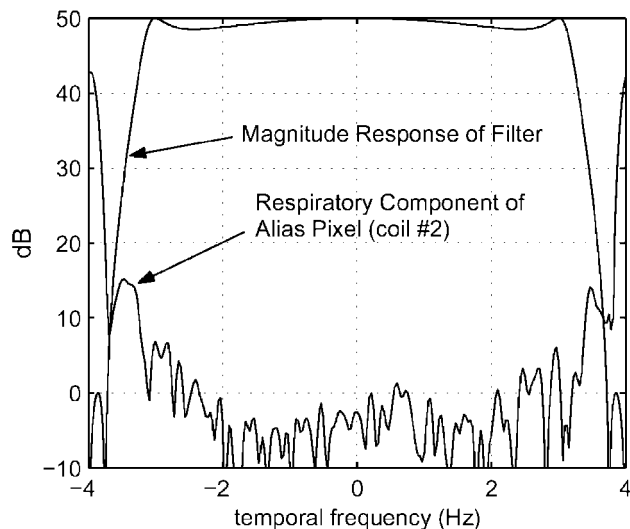


FIG. 8. Temporal spectrum of an aliased pixel with magnitude response of UNFOLD temporal filter overlaid.

application to interventional MRI: high-speed cardiac imaging and imaging during contrast agent injection. The needle position could be viewed continuously while maneuvering, as well as monitoring the injection of contrast agent. The ultimate application is to mix or molecularly bind the intended drug with the contrast agent. For instance, myocardial injection with intravascular delivery could be monitored to provide needle guidance and control of dosage.

Increased temporal resolution was achieved by means of UNFOLD interleaved *k*-space acquisition, and a low-latency temporal filter was demonstrated. This technique will be suitable for interventional MR applications when real-time reconstruction and display are implemented. Performance criteria for the rejection of alias artifacts were presented. A low-latency, recursive filter was designed and characterized for this application, and filter performance was validated experimentally.

REFERENCES

1. Lufkin RB. *Interventional MRI*. Missouri: Mosby; 1999.
2. Madore B, Glover GH, Pelc NJ. Unaliasing by Fourier encoding the overlaps using the temporal dimension (UNFOLD), applied to cardiac imaging and fMRI. *Magn Reson Med* 1999;42:813–828.
3. Pruessmann KP, Weiger M, Scheidegger MB, Boesiger P. SENSE: sensitivity encoding for fast MRI. *Magn Reson Med* 1999;42:952–962.
4. Epstein FH, Berr SS, Brookeman JR. Developments in ECG-independent retrospectively gated cardiac MRI. In: *Works in Progress for the 9th Annual Scientific Meeting and Exhibition of ISMRM*, 1990.
5. Proakis JG, Manolakis DG. *Digital signal processing principles, algorithms, and applications*. New Jersey: Prentiss-Hall; 1996. p 614–726.
6. Epstein FH, Wolff SD, Arai AE. Segmented *k*-space fast cardiac imaging using an echo-train readout. *Magn Reson Med* 1999;41:609–613.
7. Parks TW, McClellan JH. A program for the design of linear-phase finite impulse response digital filters. *IEEE Transactions on Audio and Electroacoustics* 1972;AU-20:195–199.